Effects of Re-entry and Post-Landing Heating on the Orion Crew Module Cabin Air Temperature

Stephen W. Miller[1] and Angel Alvarez-Hernandez[2]
NASA Johnson Space Center, Houston, TX 77058

A lumped-capacitance thermal model of the Orion Crew Module (CM) was developed to predict the air temperature after the vehicle had been exposed to re-entry and post-landing heating. This paper describes the initial modeling effort, the thermal environments definition, and results. The analysis considered five distinct phases: 1) a Moon-Earth transit phase to establish initial conditions, 2) a pre-entry Earth orbit, 3) re-entry through the Earth's atmosphere, 4) descent through the lower atmosphere, and 5) post-landing with the vehicle stable in the ocean after a water landing. Results from the parametric analyses showed that the air temperature in the main cabin reaches at least 42.2 °C within 2.5 hours after landing for all cases analyzed. Additionally, the main driver for the cabin air temperature is the effect of solar heating post-landing while the re-entry thermal soakback, air temperature, and sea temperature have much smaller impact on the main cabin air temperature.

Nomenclature (Miller)

$Nu_{L,BS}$	=	Length based Nusselt number for the backshell
$Nu_{D,HS}$	=	Diameter based Nusselt number for the heatshield
Re_L	=	Length based Reynolds Number
Re_D	=	Diameter Based Reynolds Number
Pr	=	Prandtl Number
Ra_D	=	Diameter Based Rayleigh Number
Ψ	=	Prandtl Number function

I. Introduction

One of the main concerns for any manned spacecraft is the safe return of the crew to the Earth's surface. In addition to surviving the harsh environments of space and re-entry through the Earth's atmosphere, the vehicle must also provide a safe haven for the occupants in the event recovery crews cannot reach the craft in a short period of time. NASA's project Orion faces the same challenge, including a requirement stating that the Crew Module (CM) must support the crew for 36-hours following a water landing with all hatches remaining closed. This paper describes the thermal model development, analysis, and results used to assess the impacts of this requirement on the current Orion design. Of specific concern is the air temperature of the cabin post-landing. The Orion Passive Thermal Control System (PTCS) Team developed analytical models to predict this temperature taking into account re-entry aerothermal loads and natural environments.

II. Model Overview

The thermal geometric model was based on the Orion 605 vehicle design. It utilized a combination of solids, surfaces, and nodes to simulate the geometry of the spacecraft in order to conduct thermal radiation analysis. Additionally, the geometric model was used to derive the thermal math model which was a lumped thermal capacitance network.

---

[1] Thermal Engineer, Thermal Design Branch (ES3), Mail Stop ES3.
[2] Thermal Engineer, Thermal Design Branch (ES3), Mail Stop ES3.

The outermost portion of the spacecraft consisted of the Thermal Protection System (TPS) as shown in Figure 1. The TPS is subdivided into a backshell, which is the conic section of the vehicle, and the heatshield, which is the spherical base and elliptical shoulder region. During re-entry, the heatshield absorbs the majority of aerothermal heating.

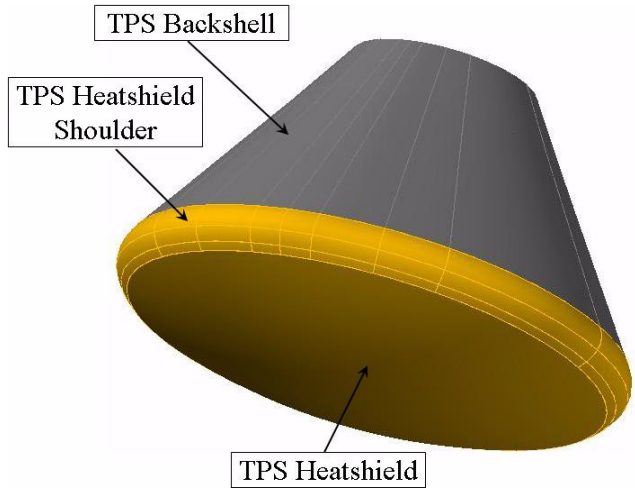

Figure 1. Geometric Math Model of TPS Surfaces

The TPS stack up consisted of different materials connected via thermal contactors. The TPS Backshell buildup consisted of an Alumina Enhanced Thermal Barrier (AETB)-8 tile (16-mm thick) bonded onto a titanium honeycomb support structure (facesheets 0.508 mm thick and core 25.4 mm thick). The main heatshield was a 79 mm thick Phenolic Impregnated Carbon Ablator (PICA) ablator bonded onto a different titanium honeycomb (1 mm thick facesheets with a 48 mm thick core). The Heatshield shoulder was a 63.5 mm thick PICA layer bonded onto a 30.5 mm thick titanium support plate.

The habitable volume of the CM is in the pressure vessel (see Figure 2). The Pressure Vessel (PV) is an aluminum lithium material which is thermally connected to the inner TPS facesheets through contactors used to represent the longerons. This contactor was assigned a value of 52.7 W/K based on hand calculations.

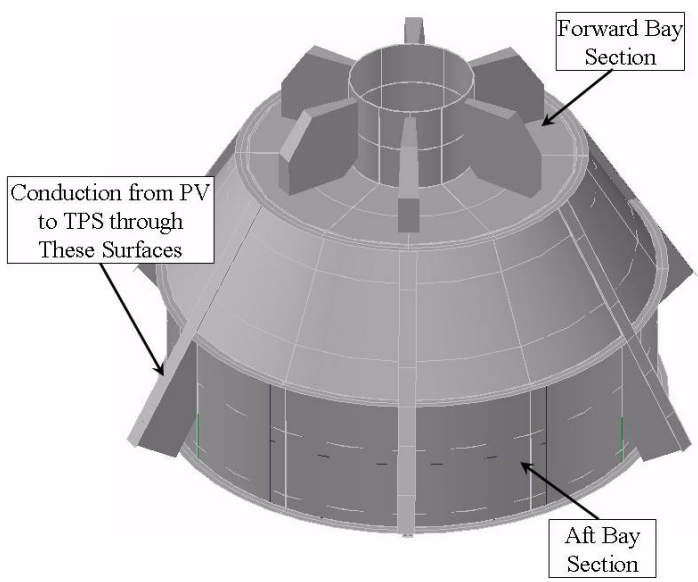

Figure 2. Geometric Math Model of CM PV

Internal to the PV, there are many avionics components modeled as single-node solid boxes with internal power dissipation. Per the power timeline used, the total pre-landing power dissipation of the vehicle was 2408.5 W and 1149.3 W post-landing. Additionally, the air volume internal to the PV was divided into five separate regions. This was done to better approximate the poor air flow between the main crew volume and the closed out areas behind panels. Figure 3 shows where these volumes are located. The air nodes were treated as diffusion nodes and assigned a mass based on the estimated volume and density. The air nodes were then thermally connected to the various structure and avionics via conductors. There was no direct thermal connection between the individual air nodes. For the main cabin air note, the area-based conductor value was 2.84 W/(m^2•K). For the remaining air nodes, the area-based conductor value was 1.42 W/(m^2•K). The difference is due to the fact that the main cabin air is actively circulated by fans while the air behind the various closeout panels is stagnant.

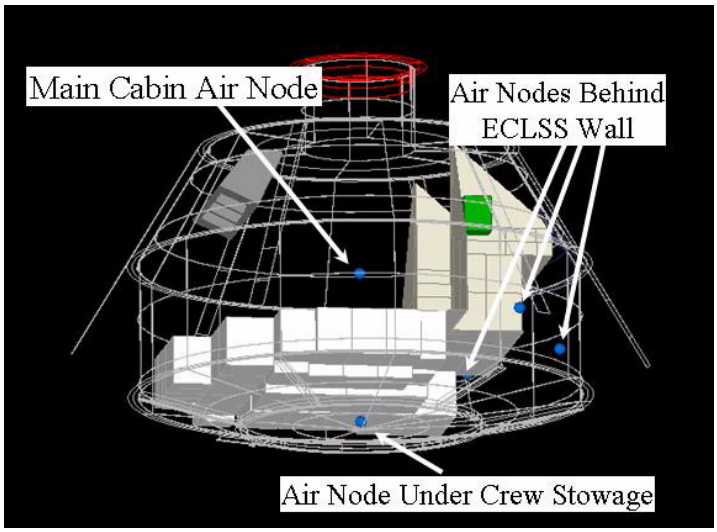

Figure 3. Location of Air Nodes in Geometric Model

III. Analysis Timeline

The analysis timeline included five distinct phases. These phases were coordinated such that the end state of one phase served as the initial conditions for the subsequent phase. The paragraphs below describe each phase in more detail.

The first phase established the initial conditions for the rest of the analysis. This phase assumed the vehicle was in an Aft-to-Sun attitude used during the transit phase between the Moon and Earth. A hot solar constant value was used, but planetary outgoing longwave radiation (OLR) and albedo were not used since it was assumed the vehicle was far enough from the Earth that these environmental heating flux sources were negligible. Because the Orion spacecraft includes both the CM and Service Module (SM) during this phase of flight, the analysis included both modules.

The second analysis phase was the pre-entry period where Orion is approaching the Earth's atmosphere. For simplicity, the analysis assumed a basic, circular orbit, but only a portion of the orbit was actually analyzed. The analysis assumed the vehicle was on the sun-side of the orbit for 1884-seconds prior to re-entry. Only the CM was included in this portion of the analysis. The vehicle was oriented such that the heatshield was on the velocity vector and hot environmental constants for solar flux, OLR, and albedo were used, see Figure 4.

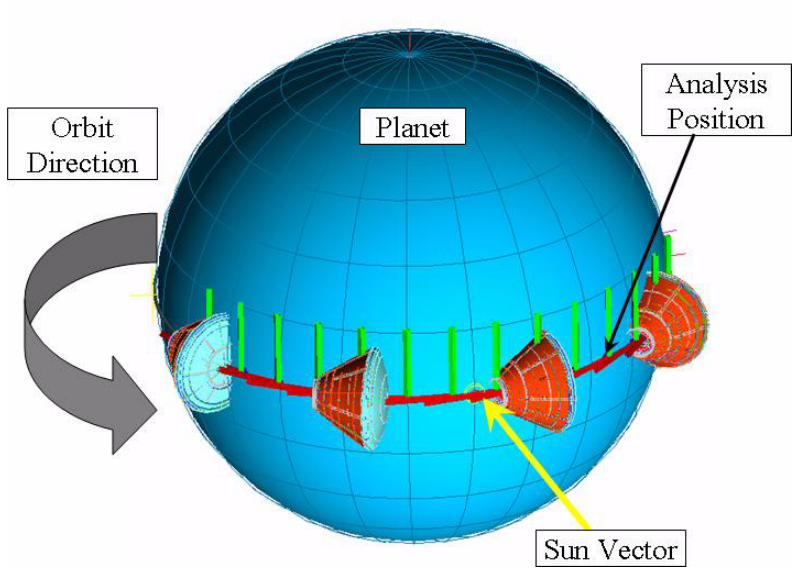

Figure 4. Pre-Entry Orbit for Analysis Phase 2

The third analysis phase was vehicle re-entry. The re-entry trajectory used was a long lunar return skip trajectory. This was selected because it provided the highest total lead load of the defined re-entry cases. This phase was 1400 seconds long. Only the CM model was used in this analysis. However, at the beginning of this phase, the main air node in the crew cabin was changed from a boundary node to a diffusion node. This was done because the vehicle's Environmental Control and Life Support architecture only allowed flow through the cabin air heat exchanger, or the crew's pressurized suits. Since the crew is in their pressure suits during re-entry, the cabin air is no longer being actively controlled to a set level. In order to properly drive the TPS temperatures, the TPS nodalization was modified to match the TPS team's breakdown. This allowed the PTCS team to use the TPS analysis results as time-dependent boundary nodes to drive the TPS nodes during re-entry. Upon completion of this phase, the TPS nodes were converted back into diffusion nodes and initialized with their final temperatures from the re-entry timeline.

The fourth phase was the crew module descent phase. During this period, convective heat transfer coefficients were applied to both the heatshield and backshell. The heat transfer from the backshell was based on flow over a flat plate, while heat transfer from the heatshield assumed flow around a sphere. The correlations[1] used were:

$$\overline{Nu}_{L,BS} = 0.029 * Re_L^{0.8} * Pr^{0.43} \tag{1}$$

$$\overline{Nu}_{D,HS} = 2 + \left(0.4 * Re_D^{0.5} + 0.06 * Re_D^{2/3}\right) Pr^{0.4} \tag{2}$$

Additionally, the CM's Forward Bay Cover was removed to accommodate the parachute deploy activities. No parachute shading was considered. A hot solar constant and sky temperature were used in accordance with the specified design environments document.

The fifth and final analysis phase was post-landing. This phase assumed the CM landed in a calm ocean with no wind. The water level was even with the heatshield shoulder and no splashing or flooding was included. While in the water, the CM heatshield transferred heat to the water and the CM Backshell transferred heat to the air via natural convection. Natural convection was chosen to minimize heat transfer to the surroundings and keep the analysis conservative. The heat transfer correlations[1] used were:

$$\overline{Nu}_{L,BS} = 0.68 + \left(0.67\left(Ra_L \Psi\right)^{1/4}\right)\left(1 + 1.6 * 10^{-8} Ra_L \Psi\right)^{1/12} \tag{3}$$

$$\Psi = \left[1 + \left(\frac{0.492}{Pr}\right)^{9/16}\right]^{-16/9} \tag{4}$$

$$\overline{Nu}_{D,HS} = 2 + \frac{0.589 Ra_D^{1/4}}{\left[1 + \left(\frac{0.469}{Pr}\right)^{9/16}\right]^{4/9}} \tag{5}$$

During the post-landing phase, a heating case was created that used a hot, ground-based solar constant, planetary OLR, and albedo. Additionally, a hot sky temperature was used for thermal radiation calculations. The sea and air temperature were assumed constant for the duration of the analysis. Figure 5 shows the post-landing thermal environment.

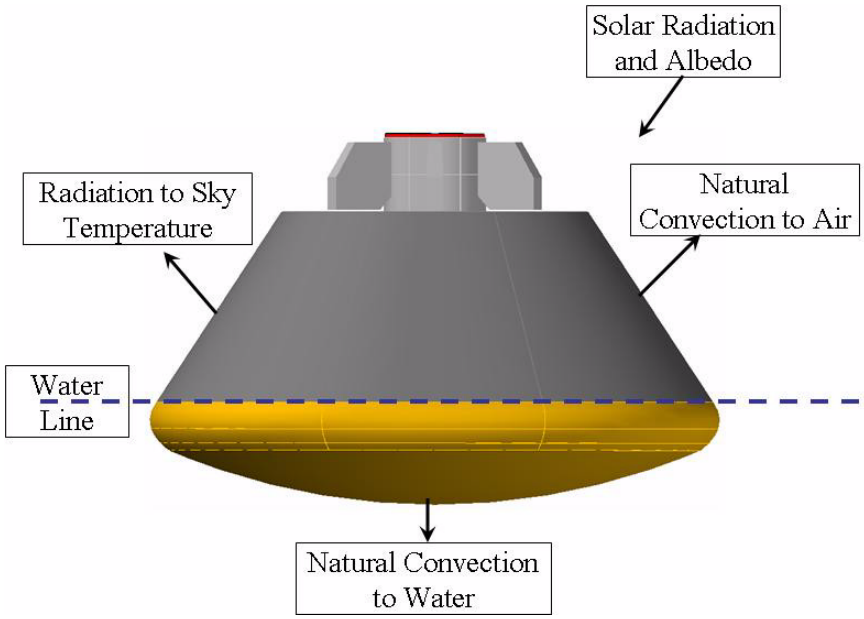

Figure 5. Thermal Environment for the Post-Landing Analysis Case

Table 1 summarizes the complete analysis timeline. To better understand the sensitivity of analysis results to the values used for the air and sea temperatures, a parametric analysis was performed over a range of expected values. The air temperature was varied between 26.7 and 35.0 °C in 2.8 °C increments. The sea water temperature was varied between 21.1 and 32.2 °C in 2.8 °C increments. Thus, a total of 20 cases were run. In all analysis cases, Time = 0 seconds corresponds to the beginning of Phase 2, the pre-entry orbit phase.

Table 1. Cabin Air Temperature Analysis Timeline

Phase Name	Order	Duration	Attitude	Solution Type
Moon-Earth Transit	1	N/A	Aft-to-Sun	Steady State
Pre-entry Orbit	2	1884 seconds	Heatshield on the velocity vector	Transient
Re-entry	3	1400 seconds	Skip Trajectory	Transient
Descent	4	383 seconds	On parachutes	Transient
Post-Landing	5	10800 seconds	Water Landing	Transient

IV. Results

Results for the main cabin air temperature are presented in Figure 6 for the case where the air temperature = 35.0 °C and the sea temperature = 32.2 °C. This case will be referred to as Case 19 in subsequent discussions and invokes the maximum water and air temperature considered in this study. Note that for the 30 minutes prior to re-

entry, the model assumed the cabin air was being actively maintained at 26.7 °C. Once this node was changed to a diffusion node during the re-entry phase, there is an initial decline in temperature which indicates the 26.7 °C boundary temperature for that node is artificially high. The main cabin air temp drops to about 23.3 °C during the initial re-entry period, but begins to rise shortly thereafter. Once the vehicle lands, the air temperature is approximately 26.7 °C again and continues to rise for the next 2.25 hours. At this point, the cabin air temperature peaks at approximately 43.9 °C. After this time, the temperature begins to decrease. This trend is seen in all of the cases analyzed.

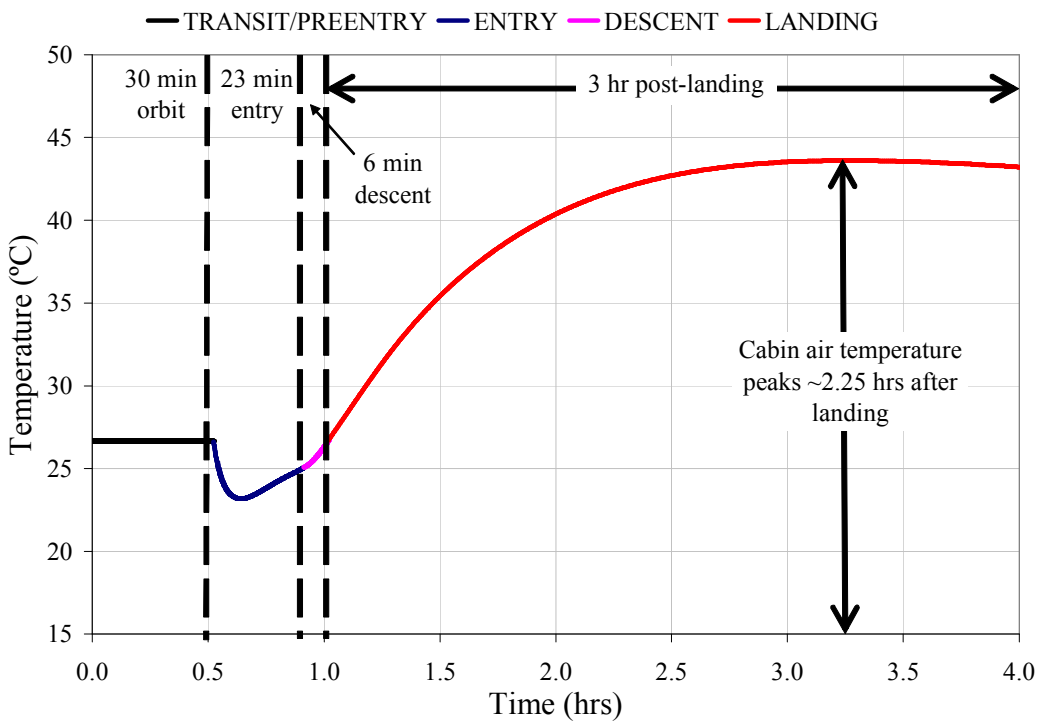

Figure 6. Cabin Air Temperature Predictions for Analysis Case 19

The peak cabin air temperature for all cases is presented in Table 2. Note that regardless of the air temperature and sea temperature, the predicted cabin air temperature is essentially the same for all cases. This implies very little dependence of the cabin air temperature on the air and sea temperatures at the landing site for the conditions assumed.

Table 2. Cabin Air Temperature Results for Varying Air and Sea Temperature Combinations

		Air Temperature (°C)			
		26.7	29.4	32.2	35.0
Sea Temperature (°C)	21.1	42.2	42.8	42.8	43.3
	23.9	42.2	42.8	43.3	43.3
	26.7	42.2	42.8	43.3	43.3
	29.4	42.2	42.8	43.3	43.3
	32.2	42.2	42.8	43.3	43.9

To assess the sensitivity of the cabin air temperature to the heat transfer from the different TPS sections, Case 19 (air temp = 35.0 °C, sea temp = 32.2 °C) was re-run with either the backshell or heatshield heat transfer coefficient set to zero for the descent and/or post-landing phases. The results from this analysis are shown in Figure 7. Note

that when heat transfer from the heatshield is eliminated during post-landing, that the cabin air temperature is predicted to exceed 71 °C for the time period analyzed. This indicates the rejection of heat from the heatshield to the sea water is a critical component in preventing soakback of thermal energy absorbed by the heatshield during re-entry into the crewed portion of the CM. In contrast, convective heat rejection from the backshell did not have a significant impact on the cabin air temperature.

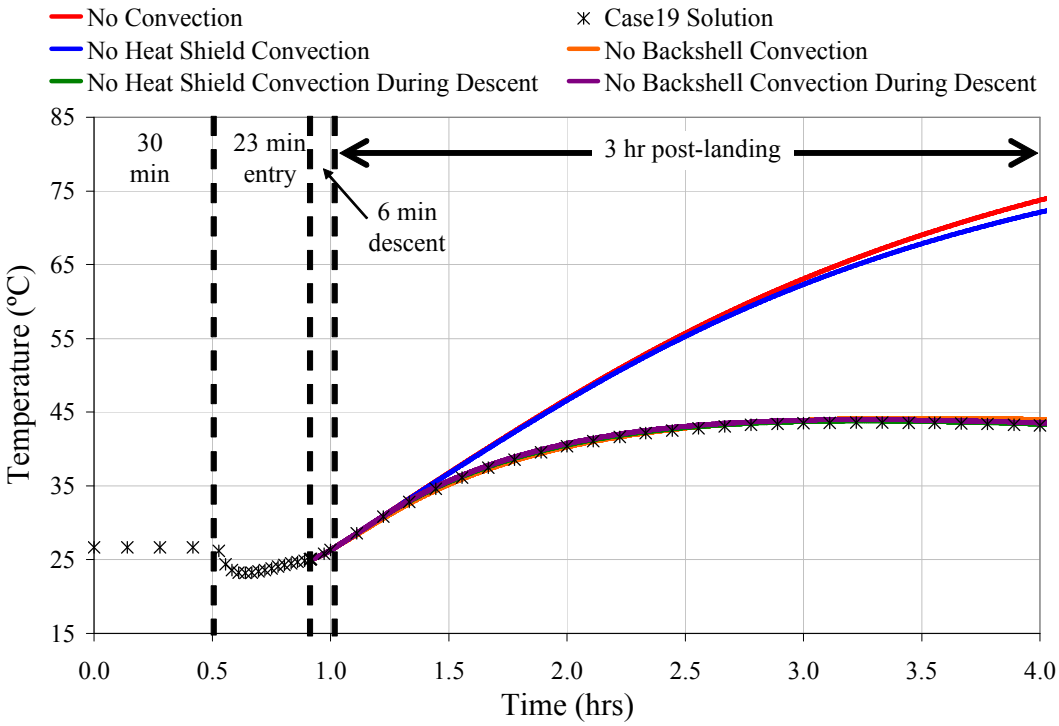

Figure 7. Effect of Convective Heat Transfer Coefficient on Cabin Air Temperature Predictions for Analysis Case 19

V. Conclusions

Based on the results presented above, it can be concluded that the main cabin air temperature is not sensitive to the air and sea temperature ranges studied in this analysis. In all analyzed cases, the cabin air temperature reached approximately 43.9 °C within 2.5 hours of landing. Additionally, the convective heat transfer from the backshell and heatshield during the descent phase (post-entry heating) also shows no significant effect on the cabin air temperature. This is mainly due to the short duration (383 seconds) of this flight phase. However, the analysis does demonstrate that the heat transfer from the heatshield to the water is critical in removing thermal energy that might otherwise soak back into the vehicle's interior.

Appendix

Natural Environments[2]

Solar Flux = 1415 W/m^2
Solar Flux during Descent = 1283 W/m^2
Solar Flux Post-Landing = 1145 W/m^2
Earth Albedo = 0.28
Earth OLR = 258.4 W/m^2

Air Properties[3]

Altitude (m)	Air Temperature (°C)	Pressure (Pa)	Density (kg/m^3)	Viscosity (Pa•s)	Sky Temperature (°C)	Thermal Conductivity (W/(m•K))
0	15.2	101325	1.225	1.79E-05	50.0	0.02536
250	13.5	98360	1.196	1.78E-05	49.7	0.02523
500	11.9	95460	1.167	1.77E-05	49.3	0.02511
750	10.3	92630	1.139	1.77E-05	49.0	0.02497
1000	8.7	89880	1.112	1.76E-05	48.6	0.02485
1250	7	87190	1.085	1.75E-05	48.3	0.02472
1500	5.4	84560	1.058	1.74E-05	47.9	0.02459
3000	-4.3	70120	0.909	1.69E-05	45.8	0.02381
4500	-14.1	57750	0.777	1.65E-05	43.7	0.02203
6000	-23.8	47220	0.660	1.60E-05	41.6	0.02223
7500	-33.5	38300	0.557	1.54E-05	39.5	0.02144
10000	-49.7	26500	0.414	1.46E-05	36.0	0.02009
12500	-56.3	17930	0.288	1.42E-05	32.5	0.01953
15000	-56.3	12110	0.195	1.42E-05	29.1	0.01953
17500	-56.3	8182	0.132	1.42E-05	25.6	0.01953
20000	-56.3	5529	0.090	1.42E-05	22.1	0.01953
25000	-51.4	2549	0.040	1.45E-05	15.1	0.01995
30000	-46.5	1197	0.018	1.48E-05	8.1	0.02036
45000	-8.8	149.1	0.002	1.67E-05	-12.8	0.02345
60000	-26	21.96	0.0003	1.58E-05	-33.8	0.02206
75000	-64.6	2.388	0.00004	1.38E-05	-54.7	0.01883

Seawater Properties[4]

Temp (°C)	Density (kg/m^3)	Viscosity (Pa•sec))	Specific Heat (kJ/(kg•K))	Conductivity (W/(m•K)))
27	1024	0.00092	3.891	0.604
32	1022	0.00082	3.883	0.613
38	1020	0.00073	3.879	0.621

References

[1]Mills, A.F. *Heat Transfer*, Richard D. Irwin, Inc., Boston, MA, 1992, Chapter 4.

[2]*Constellation Program Design Specification for Natural Environments*, NASA Document CxP 70023, 18 July 2007.

[3]Kays, W.M., and Crawford, M.E. *Convective Heat and Mass Transfer*, 3rd ed., McGraw-Hill, Inc., New York, 1993, Appendix A.

[4]U.S. Coast Guard, *Chemical Hazards Response Information System*, Chapter 6, http://www.chrismanual.com/ [cited 15 August 2007].